Title: Enhanced Respiratory Chain Supercomplex Formation in Response to Exercise in Human Skeletal Muscle.

Authors: Greggio C, Jha P, Kulkarni SS, Lagarrigue S, Broskey NT, Boutant M, Wang X, Conde Alonso S, Ofori E, Auwerx J, Cantó C, Amati F.

Journal: Cell Metabolism

Year: 2017 Feb 7

DOI: 10.1016/j.cmet.2016.11.004

Enhanced respiratory chain supercomplexes formation in response to exercise in human skeletal muscle

Running title: Supercomplexes and exercise

Authors
Chiara Greggio[1,6], Pooja Jha[2,6], Sameer S. Kulkarni[3,6], Sylviane Lagarrigue[1], Nicholas T. Broskey[1], Marie Boutant[3], Xu Wang[2], Sonia Conde Alonso[1,4], Emmanuel Ofori[1], Johan Auwerx[2], Carles Cantó[3], Francesca Amati[1,4,5*]

Affiliations
[1] Aging and Muscle Metabolism Lab, Department of Physiology, University of Lausanne, Lausanne, 1005, Switzerland
[2] Laboratory of Integrative and Systems Physiology, École Polytechnique Fédérale de Lausanne, Lausanne, 1015, Switzerland.
[3] Nestlé Institute of Health Sciences, Lausanne,1015, Switzerland.
[4] Institute of Sports Sciences (ISSUL), University of Lausanne, 1005, Switzerland
[5] Service of Endocrinology, Diabetology and Metabolism, Department of Medicine, University Hospital (CHUV), Lausanne 1011, Switzerland
[6] Shared first authorship
* Lead Contact

Corresponding authors

Francesca Amati, MD, PhD **(Lead contact)**
University of Lausanne
Bugnon 7
1005 Lausanne, Switzerland
Phone : +41 21 692 5552
Fax : +41 21 692 5505
Email : francesca.amati@unil.ch

Carles Canto, PhD
Nestlé Institute of Health Sciences
EPFL Innovation Park, Building G
1015 Lausanne, Switzerland
Phone: +41 21 6326116
Email: carlos.cantoalvarez@rd.nestle.com

Johan Auwerx, MD, PhD
Laboratory of Integrative and Systems Physiology,
EPFL, SV, Station 15,
1015 Lausanne, Switzerland
Phone: +41 21 693 9522
Fax: +41 21 693 9600
e-mail admin.auwerx@epfl.ch

Words counts
Summary words: 149

Manuscript characters: 51’896 (including spaces, references, tables and figure legends)
Figures in text: 4
Tables in text: 3
Supplemental data: 4 figures and 1 table

SUMMARY

Mitochondrial dysfunction is a hallmark of multiple metabolic complications. Physical activity is known to increase mitochondrial content in skeletal muscle, counteracting age-related decline in muscle function and protecting against metabolic and cardiovascular complications. Here, we investigated the effect of four months exercise training on skeletal muscle mitochondria electron transport chain complexes and supercomplexes in 26 healthy sedentary older adults. Exercise differentially modulated respiratory complexes. Complex I was the most upregulated complex and not stoichiometrically associated to the other complexes. In contrast to the other complexes, complex I was found almost exclusively assembled in supercomplexes in muscle mitochondria. Overall supercomplex content was increased after exercise. In particular, complex I, III and IV were redistributed to supercomplexes in the form of $I+III_2+IV$. Taken together, our results provide the first evidence that exercise affects the stoichiometry of supercomplex formation in humans and thus, reveal a novel adaptive mechanism to increased energy demand.

INTRODUCTION

Energy harvesting during oxidative phosphorylation (OXPHOS) is one of the vital functions of mitochondria. This process is carried out by the electron transport chain (ETC), a composite multiprotein system organized in four respiratory chain complexes (CI-CIV). CI-CIV oxidize reducing equivalents of NADH and $FADH_2$ generated during glycolysis, fatty acid oxidation and the tricarboxylic acid cycle, causing a proton gradient across the mitochondrial inner membrane. This chemiosmotic gradient is subsequently used by complex V (CV) to generate ATP.

The structural and functional organization of the ETC plastically changes from freely moving to super-assembled structures, called supercomplexes (SCs), and vice versa (Lapuente-Brun et al., 2013, Acin-Perez and Enriquez, 2014). Respiratory SCs were described in organisms belonging to different eukaryote kingdoms (plants, fungi and animals) (Chaban et al., 2014). SCs are principally composed of CI, CIII and CIV subunits in mammals. The contribution of CII and CV to mammalian SCs is still not clearly understood (Acin-Perez et al., 2008). Specific SCs have been identified, such as the SC $I+III_2+IV_{1-4}$ often referred to as “respirasome” (Lapuente-Brun et al., 2013, Mourier et al., 2014), as it can autonomously respire in the absence of soluble electron carriers, ubiquinone and cytochrome C, both being constitutive components of the supercomplex (Acin-Perez et al., 2008).

Although the characterization of supercomplex structure is not yet complete (Moreno-Loshuertos and Enriquez, 2016), SCs are suggested to be key importance for the stability of individual ETC complexes (Acin-Perez et al., 2008, Schagger et al., 2004, Vempati et al., 2009, Diaz et al., 2006). SCs are believed to reduce the diffusion distance required for the transfer of electrons from one complex to the other, thereby increasing the transport efficiency and limiting the production of reactive

oxygen species (Genova and Lenaz, 2014, Moreno-Loshuertos and Enriquez, 2016, Cogliati et al., 2016). Additionally, SCs have been shown to dynamically adapt to changes in cellular metabolism during fasting/feeding cycles (Acin-Perez and Enriquez, 2014) and to be stabilized by cristae shape (Cogliati et al., 2016).

The clinical relevance of SCs biology became evident with the description of the molecular origin of Barth syndrome, a fatal X-linked recessive disease characterized by cardioskeletal myopathy (Barth et al., 2004), where defective assembly of SCs correlates with severe cellular dysfunction and defects in mitochondrial bioenergetics (McKenzie et al., 2006). In other human mitochondrial diseases, genetic mutations affecting only one complex induce pleiotropic deleterious effects on other complexes, which were attributed to defective respirasome stabilization (Acin-Perez et al., 2004, Schagger et al., 2004, Ugalde et al., 2004). Alterations in SCs have also been identified in brain and muscle during aging (Frenzel et al., 2010, Lombardi et al., 2009, Lopez-Lluch et al., 2015), as well as in type 2 diabetes (Antoun et al., 2015). Although potential regulators of SCs formation, such as Cox7a2l, are currently under investigation, little is known on their physiological impact (Williams et al., 2016, Lapuente-Brun et al., 2013)

Exercise is known to promote skeletal muscle mitochondrial function and biosynthesis (Holloszy, 1967, Davies et al., 1981). While physical activity enhances mitochondrial biogenesis and respiratory capacity in aging skeletal muscle (Broskey et al., 2014, Lanza et al., 2008, Safdar et al., 2010), so far no study has examined the effect of exercise training on individual ETC complexes and SCs adaptation in human skeletal muscle, and their relationship with exercise capacity and fat metabolism during exercise.

RESULTS and DISCUSSION

Skeletal muscle ETC complexes are differentially regulated in response to exercise

In a pre/post-intervention design, twenty-six sedentary healthy men and women volunteers participated in a 16-week supervised endurance exercise training. Pre- and post-intervention characteristics are in Table 1. Exercise promoted an average increase of 45.3±8.8% mitochondrial content in *vastus lateralis*. Exercise capacity, measured by peak O_2 uptake (VO_2peak), was enhanced after intervention with an average increase of 14.7±2.6%. Exercise efficiency, i.e. the ratio of mechanical work rate over power output, measured during a 1-hour steady state acute bout of exercise at 55% of $\dot{V}O_2$ peak (Broskey et al., 2015), was also improved with an average of 23.8±3.1%. Systemic lipid oxidation during an acute bout of exercise, computed using the stoichiometric equations from Frayn (Frayn, 1983), was increased with an average of 33.4±8.7%.

The design of this study was created to highlight skeletal muscle molecular modifications with an internal validity paradigm. Each subject pre-intervention served as it's own control for post-intervention. Nevertheless, the absence of a control group may be seen as a limitation.

We first analyzed the expression of individual ETC complexes (Fig 1A). In line with the evidence that CI and CII are independent entry levels for electrons (Acin-Perez and Enriquez, 2014), their relative amounts did not correlate at baseline (Table S1). Both CI and CII positively correlated with CIII and CIV, the final acceptors of electrons in the respiratory chain (Table S1). After intervention, protein levels significantly increased compared to baseline (N=24, Fig 1B). The fold change was 2.28±0.27 for CI, 1.53±0.17 for CII, 2.06±0.24 for CIII, 1.71±0.19 for CIV, and

1.49±0.24 for CV. Change in CI did not correlate with any other complex (Fig 1C). In contrast, CII, CIII and CIV increased in response to exercise (Fig 1B) and were all positively correlated to each other (Fig 1D).

While it is well known that endurance exercise induces skeletal muscle mitochondrial biogenesis in humans (Holloszy, 1967, Davies et al., 1981, Konopka et al., 2014, Hernández-Alvarez et al., 2010). Here, we document a striking regulation of respiratory chain complexes after 4 months of exercise intervention confirming that the expression of the ETC complexes is increased in response to physical activity in human skeletal muscle mitochondria, and illustrate how the magnitude of the response differs between complexes. These differential changes in individual ETC complexes suggest the possibility for multiple regulatory layers of respiratory chain adaptations to physical training.

Transcripts encoding ETC components depicted only moderate modifications with intervention (Fig 1E). These observations are coherent with the time course observations that mRNA responses to acute bouts of exercise follow pulsatile transient increases, which lead to elevated protein content after periods of exercise training (Egan et al., 2013) and with a recent transcriptomics-proteomics multilayer approach study (Williams et al., 2016).

Supramolecular organization of CI-CV into SCs in human skeletal muscle

Supramolecular organization of CI-CV in SCs in human skeletal muscle was assessed by blue native polyacrylamide gel electrophoresis (BN-PAGE) of mitochondrial extracts using digitonin solubilization (Schagger et al., 2004, Jha et al., 2016a) before and after intervention. Using the most recent description and characterization of SCs structure in mammalian tissues (Moreno-Loshuertos and Enriquez, 2016), we labeled with details the specific SCs following the nomenclature

previously described in human tissues (Schagger, 2002, Schagger et al., 2004, Sun et al., 2016) (Fig 2A).

In line with previous reports (Schagger et al., 2004, Moreno-Lastres et al., 2012) and data in human muscle (Antoun et al., 2015), CI was mostly found in superassembled species (95.19±3.25% in SCs). CII existed predominantly, but not exclusively, as a single band and was not detected in SCs. CIII and CIV existed both as free and as superassembled species. CIII was equally distributed in free and SC pools (53.88±1.58% in SC), while CIV was predominantly found in the free form (only 19.97±6.11% in SCs). As for CV, it was mostly detected in 4 oligomeric states, as previously observed (Acin-Perez et al., 2008, Dudkina et al., 2010).

The overall content of SCs was increased after exercise, as evidenced in immunoblots using an OXPHOS antibodies cocktail (Fig 2B, N=17). Quantification allowed to observe a significant change with intervention of +49.97%±17.72 (Fig 2C).

In order to demonstrate that all subunits of each of the complexes are represented in the representative blots, we performed mass spectrometry based proteomic analysis from 7 successively cut BN-PAGE gel bands, which represent all the complexes and SCs (Fig S1A). More than ~85% of the proteins for each subunit were detected for each band (Fig S1B).

Exercise redistributes individual complexes in favor of SC I+III$_2$+IV$_n$

We next evaluated the assembly of CI, CIII and CIV separately in the SCs in 9 subjects (Fig S2). Indeed, due to the scarcity of muscle biopsies, we could not perform these analyses in more subjects. Exercise significantly increased the amounts of CI, CIII and CIV included in the SCs suggesting that all of them contributed to increasing total SCs content (Fig 3A).

While the most predominant SCs in human skeletal muscle have been described as SC $I+III_2+IV_1$ and SC $I+III_2$ (Schagger, 2002, Schagger et al., 2004), as seen and labeled in figure 2A, a recent paper from Sun et al. (Sun et al., 2016) describes SC $I_n+III_n+IV_n$ in human cells and cell lines derived from human tissues. This was also confirmed in rat brain by a very recent publication of Muller et al. using a novel method linking blue native gels with mass spectrometry (Muller et al., 2016). Thus, for further analyses, we opted to use a conservative approach, similarly used in a recent publication (Perez-Perez et al., 2016): we covered SC $I+III_2+IV_1$ within the nomenclature of SC $I+III_2+IV_n$ due to the fact that we detected more than one band positive for CI, CIII and CIV, which may be explained by additional copies of CIV together with SC $I+III_2$. Following this criteria, we observed a significantly higher content of CI, CIII and CIV in SC $I+III_2+IV_n$ after the exercise intervention (respectively +51.41±15.87%, +54.91±10.23% and +244.58±64.80%, all $p<0.05$).

Since individual complexes are differentially allocated to “free” or “superassembled” pools (Althoff et al., 2011 , Dudkina et al., 2010, Schagger and Pfeiffer, 2000), we next computed the proportion of each complex in the SCs. Exercise training promoted a redistribution of CIII and CIV into SCs (Fig 3B). This was not the case for CI, as it was already predominantly allocated to SCs before intervention. The preferential assembly of CI into SCs, even at baseline, could be a specific feature of human skeletal muscle, as its free active form is present in murine heart and liver (Lapuente-Brun et al., 2013, Mourier et al., 2014 , Williams et al., 2016). This might critically determine human ETC biology, as CI is known to be the most unstable ETC complex and a major site of reactive oxygen species (ROS) production together with CIII (Maranzana et al., 2013). We hypothesize that CI regulation could preferentially take place at the level of the “total” amount, more than

at the “assembly” level, thus explaining why CI was so strongly induced at the protein level compared to the other ETC complexes. This coincides with a recent proposal from Guaras and al. (Guaras et al., 2016).

We next examined whether any particular SCs assembly would be differentially induced by exercise. Therefore we analyzed the distribution of individual species before and after intervention by evaluating the percentages of each species over the total detected signal (Fig 3C). We observed that the fraction of CI allocated to SC $I+III_2+IV_n$ was increased after intervention, while the fraction of CI in SC $I+III_2$ was decreased. Similarly, the fraction of CIII was increased in SC $I+III_2+IV_n$, SC III_2+IV and HMW species SC I_n+III_n, while it was decreased in the free pool and SC $I+III_2$. Likewise, the faction of CIV allocated to SC $I+III_2+IV_n$ and SC III_2+IV increased at the expense of the free pool (IV and IV_2) which was significantly decreased (Fig 3C). Correlative analyses revealed that CIII displays a strong inverse association between the increase of CIII fraction in the SC $I+III_2+IV_n$ and the decrease in its free pool (Fig 3D). The relationship appeared even stronger between free CIII and CIII within total SCs (defined as the sum of SC $I+III_2+IV_n$ + HMW SC I_n+III_n + SC III_2+IV_2). Similar results were obtained when comparing the relative changes in CIV pools. Further, the decrease in SC $I+III_2$ relative fraction was observed for both CI and CIII, and was strongly correlated among each other, suggesting a tight inter-regulation of the two complexes for this specie.

Taken together, our results show that physical activity not only induces SCs assembly in skeletal muscle mitochondria, but it also preferentially favors the SC $I+III_2+IV_n$, as well as the functional but not fully super-assembled SC III_2+IV. These higher-order SCs are induced at the expense of free complexes or lower molecular weight species.

Exercise capacity, efficiency and reliance on fat are related to specific SCs assemblies

At baseline, CIII and CIV content in the SCs pool correlated with physical fitness measured by peak oxygen uptake (VO_2peak) (Fig 3E). In addition, the greater the fraction of CIV in SCs the greater was exercise efficiency (i.e. the ratio of mechanical work rate over energy expenditure (Broskey et al., 2015))(Fig 3E). Inversely, free CIV was negatively associated with VO_2 peak and efficiency (Fig 3E). Further, the amount of CIII in the respirasome fraction was associated with steady state exercise fat oxidation, testifying for a possible role of SCs for efficient energy use during endurance exercise (Fig 3E).

Relationships between changes with intervention of ETC complexes in SCs $I+III_2+IV_n$, or in the free pool, and changes in exercise data are presented in table 2. Strong opposite associations are observed between the changes in fractions of CIII and CIV allocated to SC $I+III_2+IV_n$ and their free form with markers of exercise capacity and efficiency. Increased reliance on fat as a substrate for submaximal exercise, a known adaptation to training (Amati et al., 2008), was also related with reductions in the fraction of free CIII.

Functional relevance of SCs in human skeletal muscle

Seven independent biopsy specimens were used to assess functional relevance of SCs. For this purpose, we performed high resolution respirometry analyses (O2K Oxygraph; Oroboros Instruments, Innsbruck, Austria) in permeabilized muscle fibers (Fig 4A-B). In parallel, we analyzed SCs levels from the same biopsies through BN-PAGE (Fig 4C-D). While respirometry analyses required fresh tissue, SCs content were similarly detectable in fresh and frozen tissue (Fig S3).

Maximal O_2 consumption was positively related to the amount of SCs as well as to the amount of each complex CI, CIII and CIV in the SCs (Fig 4E). This was also true for State 3 respiration using both CI and CII substrates (Table 3). When looking at the proportions of free vs. superassembled complexes, opposite relationships were observed. Further, all these relationships were inverted with State 2 respiration, which reflects respiratory leaks (Makrecka-Kuka et al., 2015, Pesta and Gnaiger, 2012). Overall, these results suggest that respiratory coupling capacity is correlated with SCs formation.

Interestingly, in contrast with our previous work in mice models where State 3 respiration through Complex I accounts for almost maximal respiration capacity (Boutant et al., 2015), this was not the case in human skeletal muscle. Indeed, State 3 CI-linked respiration ranged from 55 to 81% of maximal respiratory capacity (mean 70±0.1%). This shows that Complex I does not saturate the electron transport system capacity through Complexes III and IV in permeabilized human skeletal muscle. Further, it reinforces the fact that data from mouse models should be carefully evaluated when extrapolating to human skeletal muscle mitochondrial physiology. This has to be taken even more carefully when using the C57Bl/6 mice, the most common strain for metabolic studies. This strain carries a mutation in the *Cox7a2l* gene, which leads to the expression of a short, unstable variant of the COX7A2L. This protein (also known as the Supercomplex Assembly Factor I (SCAFI), in turn, is a supercomplex-specific factor responsible for the dynamic association of complex IV into these structures (Williams et al., 2016, Lapuente-Brun et al., 2013).

It is currently not known if the recruitment of individual complexes in SCs is instrumental to improve the mitochondrial reserve respiratory capacity, defined as the difference between ATP production at basal and at maximal respiration. Our results

suggest that this could be indeed the case since exercise elicits improved SCs and has been shown to improve maximal respiratory capacity (Holloszy, 1967, Phielix et al., 2010). Further supporting this scenario, changes in SCs were related to improvements in exercise capacity in our cohort, as well as with changes in better efficiency and increased fat oxidation during an acute submaximal exercise. Although purely observational our data on respiration confirms the existence of strong relationships between the different components of mitochondrial respiration and SCs content.

Activity of the ETC is enhanced in response to exercise

BN-PAGE in gel activity assays for CIV and CI before and after intervention were performed from five subjects from whom enough frozen biopsy material was available. Although this data is not quantitative, and CI activity is masked by CIV activity, an overall increase in CIV and (CIV+CI) activity was observed after the exercise intervention (Fig S4). In particular, stronger activity was detected in the HMW SCs, proving that these species are functional respiratory units.

CONCLUSION

The physiological implication of SCs assembly has sparsely been studied in humans (Antoun et al., 2015), this is the first time that response to exercise has been investigated. We show that the amount of superassembled complexes is increased in response to exercise. Further, exercise promoted the redistribution of CI from SC I+III_2 to SC I+III_2+IV_n. Exercise preferentially favored the re-distribution of CIII and CIV to functional SCs species as the fully assembled SC I+III_2+IV_n, at the expenses of free or other SCs, such as SC I+III_2. These observations reinforce the “plasticity”

model, which suggests that free and superassembled complexes co-exist and are recruited in response to the energy demand.

The physiological significance of respiratory SCs formation is still not well understood. Recent evidences suggest that there might exist different CoQ pools, differently dedicated to reducing equivalents coming from either NADH or $FADH_2$ (Lapuente-Brun et al., 2013). By modulating the ultrastructural assembly of complexes I and III, we might enhance the ability of using reducing equivalents from NADH during muscle contraction. Respiratory SCs have also been suggested to accelerate electron transport, preventing this way the generation of ROS (Ghelli et al., 2013, Maranzana et al., 2013). This way, increased SCs assemblies might be important to ensure that high electron transport fluxes during exercise training do not translate into damaging amounts of ROS.

Given that mitochondrial dysfunction is associated with both aging (Short et al., 2005) and metabolic disorders (Andreux et al., 2013, Kim et al., 2008), it will be interesting to evaluate whether the changes in SCs assembly are also instrumental for the therapeutic benefits of exercise on glucose handling and age-related physiological decline. Recently alterations in SCs assembly in diabetic obese individuals have been reported (Antoun et al., 2015).

In conclusion, we demonstrate that the human skeletal muscle respiratory chain is profoundly affected by 4 months of endurance exercise, not only in total content of individual complexes, but also in the way they assemble into SCs. These modifications were accompanied with functional and physiological improvements.

EXPERIMENTAL PROCEDURES

Subjects characteristics

Twenty-six sedentary men and women where recruited for this study (Table 1). Subjects had to be between 60 and 80 years old, in good general health and weight stable. They were acknowledged as sedentary, if doing less than one exercise session per week. Active smoking, diabetes and pharmacological treatments known to affect glucose homeostasis were among the exclusion criteria. The Ethics committee of the Canton of Vaud approved the study protocol. Each participant gave written informed consent before starting the study.

Clinical study design

In a pre-/post-intervention design, subjects were phenotyped at baseline and after intervention. Height was measured using a wall-mounted stadiometer and weight using a calibrated medical digital scale (Seca GmBh, Hamburg, Germany). Physical fitness was determined by VO_2peak using a graded exercise test on an electronically braked cycle ergometer (Lode B.V, Groningen, Netherlands). Oxygen consumption was computed via indirect calorimetry (Metalyzer3B; Cortex, Leipzig, Germany). The protocol was suited for older volunteers of various degrees of fitness (Amati et al., 2011, Broskey et al., 2014). Acute exercise efficiency and fat oxidation were measured during a one hour submaximal steady state exercise bout as previously described (Amati et al., 2008, Broskey et al., 2015).

Intervention

The exercise training consisted of a 16-week supervised (3 sessions/week), moderate-intensity aerobic protocol described in details elsewhere (Broskey et al., 2014). Frequency, duration, and volume of exercise were tightly monitored. The volunteers were asked to follow their typical diet during the study.

Skeletal muscle biopsy

Percutaneous muscle biopsies from the *vastus lateralis* were collected after an overnight fast in tight controlled conditions (Broskey et al., 2014). Subjects were requested not to exercise in the last 48 hours. After trimming with a dissecting microscope (MZ6; Leica Microsystems, Wetzlar, Germany), one portion of the specimen (5 mg) was fixed and the remaining specimen was flash frozen in liquid nitrogen and stored at −80°C. For 7 specimen, 50-100mg were used fresh for high resolution respirometry.

Mitochondrial content

Transmission electron microscopy was used to measure mitochondrial volume density as a marker of mitochondrial content. This stereological method has been described in details elsewhere (Broskey et al., 2013).

Gene expression analysis

Total mRNA preparations, cDNA synthesis, and quantitative RT-PCR were performed as described previously (Broskey et al., 2014). Primers used were: ATP5g1 (F:AGCAGGGGTTGCAGGGTAGT; R:CTGGCCACCTGGAGTGGGAAGT); Ndufa2 (F:CAAGCTCTGGGCCCGCTACG; R:CCCAGGCTCTGGGGCTGTTG); b-Actin (F:TCGTGCGTGACATTAAGGAG; R:GTCAGGCAGCTCGTAGCTCT) and Cyclophyllin (F.CTTCCCCGATGAGAACTTCAAACT; R:CACCTCCATGCCCTCTAGAACTTT).

Western blotting

Skeletal muscle samples were lysed in lysis buffer (50 mM Tris-HCL pH7.5, 150 mM NaCl, EDTA 5 mM, NP40 1%, sodium butyrate 1mM, protease inhibitors). Proteins were quantified using BCA assay (Pierce, Waltham, MA). 15-20 µg of total proteins were separated by SDS-PAGE and transferred onto nitrocellulose

membranes. Membranes were blocked with 5% BSA prepared in TBST and incubated overnight with antibodies against target proteins.

Antibodies used for western blotting were against NDUFA9 (CI subunit, Mitosciences, Ab14713, dil.1:2000, Abcam, Cambridge, UK), SDHA (CII subunit, Abcam, Ab14715, dil. 1:5000), UQCRC1 (CIII subunit, Abcam, Ab110252, dil. 1:2000), MTCO1 (CIV subunit, Abcam, Ab14745, dil. 1:1000), ATP5A (CV subunit, Abcam, Ab14748, dil. 1:5000), α tubulin (Sigma, T9026, dil. 1:5000, St Louis, MS).

Protein expression was determined by ECL (Amersham, UK) and by exposing on X-ray films. Respective bands were quantified by ImageJ software (NIH, Bethesda, MD).

Mitochondria isolation

Mitochondrial isolation was performed using an established protocol (Jha et al., 2016b). 90mg of skeletal muscle biopsy specimen were homogenized in 2ml cold IB. Homogenization was achieved at maximum speed after 20 strokes. Following 2 rounds of centrifugation at 600x g for 10 min, the mitochondrial fraction was washed and pelleted at 7000xg for 10 min. The pellet was suspended in ~150µl cold IB and stored at -80C in 30µg aliquots. Pre and post samples from the same subject were extracted and quantified in batches to minimize technical variability. Figure S3 presents the confirmation that these extracts retain function and structure.

SC detection, identification and quantification

SC detection, identification and quantification was performed using an established protocol (Jha et al., 2016b). *SC detection (N=17):* 30µg mitochondrial extracts were solubilized with digitonin at the final concentration of 8.7g/g of protein. After 30-minutes incubation in ice, the clear supernatant was loaded in 15-wells 4-13% BN gels (Invitrogen) in a SureLock Xcell tank (Invitrogen), run and transferred

(Jha et al., 2016b). Simultaneous detection of CI-CV was achieved with the anti-OXPHOS complex kit (Invitrogen, 457999, dil 1:1000) complemented with an anti-MTCO1 (CIV subunit, Abcam, 14705, dil 1:2000). When possible, technical replicates were performed (N=14/17).

SC identification (N=9) **:** 30µg mitochondrial extracts (with digitonin 8.7g/g of protein and G-250 Blue Coomassie) were individually loaded for the detection of each complex. After the transfer, the membrane was cut and incubated the same primary antibodies used for western blotting, with the exception of anti-COX5b (CIV subunit, Protein Tech, 11418-AP, dil 1:1000). Mouse (CI-CIII, CV) and Rabbit (CIV) Western Breeze Chromogenic Immunodetection Kits were used.

Image analysis and Quantification: Images were acquired at 1200dpi with a HP Scanjet J4050 scanner and converted to 16-bit with ImageJ. Quantification was executed with the function Analyze/gel/Plot lanes. The peaks were selected and quantified from the plots (Fig S2).

BN-PAGE in gel activity

BN-PAGE in gel activity was performed as described elsewhere with minor modifications (Jha et al., 2016b). 120µg mitochondrial extracts (solubilized with digitonin 8g/g of protein) were loaded in 10-wells 4-13% gels (Invitrogen) and run with chilled buffers in ice (Jha et al., 2016b). First the gel was incubated in CIV substrate (25 mg of 3,3'-Diamidobenzidine tetrahydrochloride (DAB); 50 mg cytochrome c; 45 mL of 50 mM phosphate buffer pH 7.4 and 5 mL water) for 40 min. The gel was scanned and then incubated in 20 ml of CI substrate (2 mM Tris-HCl pH 7,4; 0,1 mg/ml NADH; 2,5 mg/ml Nitrotetrazolium Blue chloride) for 20 min. Reaction was stopped with 10% of acetic acid for 10 min followed by washing and scanning.

High resolution respirometry

High-resolution respirometry experiments were performed as previously described (Boutant et al., 2015). Briefly, after dissection, the fresh biopsy was placed into relaxing buffer (in mM: 2.8 Ca_2K_2EGTA, 7.2 K_2 EGTA, 5.8 ATP, 6.6 $MgCl_2$, 20 taurine, 15 Na_2 phosphocreatine, 20 imidazole, 0.5 dithiothreitol, and 50 MES, pH 7.1) and trimmed of surrounding epithelial and fat tissue. Then, the biopsy was gently separated into small fiber bundles. Then, muscle fibers were permeabilized in relaxing buffer supplemented with 0.005% (wt/vol) saponin for 20 minutes. The tissue was then equilibrated in respirometry medium [in mM: 0.5 EGTA, 3 $MgCl_2$, 60 K-lactobionate, 20 taurine, 10 KH_2PO_4, 20 HEPES, 110 sucrose and 0.1% (wt/vol) bovine serum albumin, pH 7.1]. Thereafter, 1-3 mg of permeabilized fibers were placed on the respirometry chamber. O_2 flux was initially measured by adding malate (2 mM), pyruvate (10 mM) and glutamate (10 mM), in the absence of ADP (Sate 2 - CI). State 3 respiration using Complex I substrates (State 3 – CI) was then achieved by the addition of ADP (5 mM). This was followed by the addition of succinate (10 mM) in order to achieve State 3 respiration driven by both Complex I and Complex II substrates (State 3 - CI+CII). Next, carbonylcyanide-4-(trifluoromethoxy)-phenyl-hydrazone (FCCP) was titrated to evaluate maximum flux through the electron transfer system. In general, 0.5 µM FCCP allowed reaching maximal O_2 consumption rates in permeabilized human muscle fibers. Finally, antimycin A (2.5 µM) was added to block Complex III and verify that O_2 consumption rates were due to mitochondrial respiration. O_2 flux values are expressed relative to tissue wet weight per second. Flux control ratios, the relative contribution of the different respiration parameters to maximal electron flux through the electron transport system, were calculated by dividing each value by maximal respiratory capacity (FCCP).

Statistical analysis

Unless specified otherwise all values presented in the text are mean ± SEM. Intervention effect was determined either with paired T test if the normality assumption was met or Wilcoxon signed rank test if normality was not met. Significance level was set a priori at 0.05. All statistical analyses were performed using JMP version 11 (SAS Institute, Cary, NC). Graphs were done using Prism version 5 for PC (GaphPad Inc, La Jolla, CA).

SUPPLEMENTAL INFORMATION

Supplemental Information includes four figures, one table and supplemental experimental procedures and can be found with this article online at….

AUTHORS CONTRIBUTIONS

Conceptualization: F.A., C.C. and J.A.; Methodology: F.A., C.C., and P.J.; Formal analysis: C.G.; Investigation: C.G., P.J., S.S.K., S.L., M.B., N.T.B., X.W., S.C.A., E.O., C.C., F.A.; Co-first authors specific contributions: C.G. isolated mitochondria, performed BN gels, analyzed the data, performed statistical analyses and drafted the manuscript. P.J. developed the BN gels methodology and adapted their use to humans, performed BN gels, analyzed the data, edited the manuscript. S.S.K. performed WB and respirometry analyses, analyzed the data, and edited the manuscript. Resources: F.A., C.C., J.A.; Data curation: C.G., F.A.; Writing – original draft: C.G. and F.A.; Writing – Review & Editing: P.J., S.S.K., C.C. and J.A., Visualization: C.G., P.J. and S.L.; Supervision: F.A., C.C., J.A.; Project administration: F.A.; Funding acquisition: F.A. and J.A.; Co-senior authors: F.A., C.C., J.A. are designated as 3 co-PIs as this work has been conducted in a collaboration across their 3 labs. J.A. supervised P.J and in particular the development and analysis of BN gels, J.A. also supervised X.W. . C.C. supervised S.S.K. and M.B, and also performed respirometry. F.A. designed and created the

study, organized and led the clinical intervention, performed all medical testing including biopsies and stress tests, and supervised C.G., S.L., N.T.B., S.C.A and E.O.

ACKNOWLEDGMENTS

All three labs are part of the Lausanne Integrative Metabolism & Nutrition Alliance (LIMNA). We thank our research volunteers, the nursing staff of the Clinical Research Center of the University Hospital of Lausanne, and Cyril Besson in the exercise lab. Thank you to Jean Daraspe and Bruno Humbel from the Electron Microscopy Facility of the University of Lausanne. We also thank Manfredo Quadroni at the Protein Analysis Facility of the University of Lausanne.

This study was supported by the Swiss National Science Foundation (SNSF) (Ambizione PZ00P3-126339, PZ00P3-149398 and 320030_170062), grants from the Leenaards Foundation and BASPO (all to F.A.). J.A. is the Nestlé Chair in Energy Metabolism and work in his laboratory was supported by the EPFL, NIH (R01AG043930), Systems X (SySX.ch 2013/153) and SNSF (31003A-140780).

DISCLOSURES

S.S.K., M.B. and C.C. are employees of the Nestlé Institute of Health Sciences SA. Other authors have nothing to disclose.

REFERENCES

Acin-Perez, R., Bayona-Bafaluy, M. P., Fernandez-Silva, P., Moreno-Loshuertos, R., Perez-Martos, A., Bruno, C., Moraes, C. T. & Enriquez, J. A. (2004). Respiratory complex III is required to maintain complex I in mammalian mitochondria. *Mol Cell,* 13**,** 805-15.

Acin-Perez, R. & Enriquez, J. A. (2014). The function of the respiratory supercomplexes: the plasticity model. *Biochim Biophys Acta,* 1837**,** 444-50.

Acin-Perez, R., Fernandez-Silva, P., Peleato, M. L., Perez-Martos, A. & Enriquez, J. A. (2008). Respiratory active mitochondrial supercomplexes. *Mol Cell,* 32**,** 529-39.

Althoff, T., Mills, D. J., Popot, J. L. & Kuhlbrandt, W. (2011). Arrangement of electron transport chain components in bovine mitochondrial supercomplex I1III2IV1. *EMBO J,* 30**,** 4652-64.

Amati, F., Dube, J. J., Alvarez-Carnero, E., Edreira, M. M., Chomentowski, P., Coen, P. M., Switzer, G. E., Bickel, P. E., Stefanovic-Racic, M., Toledo, F. G. & Goodpaster, B. H. (2011). Skeletal muscle triglycerides, diacylglycerols, and ceramides in insulin resistance: another paradox in endurance-trained athletes? *Diabetes,* 60**,** 2588-97.

Amati, F., Dube, J. J., Shay, C. & Goodpaster, B. H. (2008). Separate and combined effects of exercise training and weight loss on exercise efficiency and substrate oxidation. *J Appl Physiol,* 105**,** 825-31.

Andreux, P. A., Houtkooper, R. H. & Auwerx, J. (2013). Pharmacological approaches to restore mitochondrial function. *Nat Rev Drug Discov,* 12**,** 465-83.

Antoun, G., Mcmurray, F., Thrush, A. B., Patten, D. A., Peixoto, A. C., Slack, R. S., Mcpherson, R., Dent, R. & Harper, M. E. (2015). Impaired mitochondrial oxidative phosphorylation and supercomplex assembly in rectus abdominis muscle of diabetic obese individuals. *Diabetologia*.

Barth, P. G., Valianpour, F., Bowen, V. M., Lam, J., Duran, M., Vaz, F. M. & Wanders, R. J. (2004). X-linked cardioskeletal myopathy and neutropenia (Barth syndrome): an update. *Am J Med Genet A,* 126A**,** 349-54.

Boutant, M., Joffraud, M., Kulkarni, S. S., Garcia-Casarrubios, E., Garcia-Roves, P. M., Ratajczak, J., Fernandez-Marcos, P. J., Valverde, A. M., Serrano, M. & Canto, C. (2015). SIRT1 enhances glucose tolerance by potentiating brown adipose tissue function. *Mol Metab,* 4**,** 118-31.

Broskey, N. T., Boss, A., Fares, E. J., Greggio, C., Gremion, G., Schluter, L., Hans, D., Kreis, R., Boesch, C. & Amati, F. (2015). Exercise efficiency relates with mitochondrial content and function in older adults. *Physiol Rep,* 3.

Broskey, N. T., Daraspe, J., Humbel, B. M. & Amati, F. (2013). Skeletal muscle mitochondrial and lipid droplet content assessed with standardized grid sizes for stereology. *J Appl Physiol (1985),* 115**,** 765-70.

Broskey, N. T., Greggio, C., Boss, A., Boutant, M., Dwyer, A., Schlueter, L., Hans, D., Gremion, G., Kreis, R., Boesch, C., Canto, C. & Amati, F. (2014). Skeletal muscle mitochondria in the elderly: effects of physical fitness and exercise training. *J Clin Endocrinol Metab,* 99**,** 1852-61.

Chaban, Y., Boekema, E. J. & Dudkina, N. V. (2014). Structures of mitochondrial oxidative phosphorylation supercomplexes and mechanisms for their stabilisation. *Biochim Biophys Acta,* 1837**,** 418-26.

Cogliati, S., Enriquez, J. A. & Scorrano, L. (2016). Mitochondrial Cristae: Where Beauty Meets Functionality. *Trends Biochem Sci,* 41**,** 261-73.

Davies, K. J., Packer, L. & Brooks, G. A. (1981). Biochemical adaptation of mitochondria, muscle, and whole-animal respiration to endurance training. *Arch Biochem Biophys,* 209**,** 539-54.

Diaz, F., Fukui, H., Garcia, S. & Moraes, C. T. (2006). Cytochrome c oxidase is required for the assembly/stability of respiratory complex I in mouse fibroblasts. *Mol Cell Biol,* 26**,** 4872-81.

Dudkina, N. V., Kouril, R., Peters, K., Braun, H. P. & Boekema, E. J. (2010). Structure and function of mitochondrial supercomplexes. *Biochim Biophys Acta,* 1797**,** 664-70.

Egan, B., O'connor, P. L., Zierath, J. R. & O'gorman, D. J. (2013). Time course analysis reveals gene-specific transcript and protein kinetics of adaptation to

short-term aerobic exercise training in human skeletal muscle. *PLoS One,* 8**,** e74098.
Frayn, K. N. (1983). Calculation of substrate oxidation rates in vivo from gaseous exchange. *J Appl Physiol,* 55**,** 628-34.
Frenzel, M., Rommelspacher, H., Sugawa, M. D. & Dencher, N. A. (2010). Ageing alters the supramolecular architecture of OxPhos complexes in rat brain cortex. *Exp Gerontol,* 45**,** 563-72.
Genova, M. L. & Lenaz, G. (2014). Functional role of mitochondrial respiratory supercomplexes. *Biochim Biophys Acta,* 1837**,** 427-43.
Ghelli, A., Tropeano, C. V., Calvaruso, M. A., Marchesini, A., Iommarini, L., Porcelli, A. M., Zanna, C., De Nardo, V., Martinuzzi, A., Wibrand, F., Vissing, J., Kurelac, I., Gasparre, G., Selamoglu, N., Daldal, F. & Rugolo, M. (2013). The cytochrome b p.278Y>C mutation causative of a multisystem disorder enhances superoxide production and alters supramolecular interactions of respiratory chain complexes. *Hum Mol Genet,* 22**,** 2141-51.
Gnaiger, E. 2014a. *Mitochondrial pathways and respiratory control - the blue book,* Innsbruck, Oroboros.
Gnaiger, E. 2014b. *MitoPedia* [Online]. Available: http://www.bioblast.at/index.php/MitoPedia [Accessed August 30 2016].
Guaras, A., Perales-Clemente, E., Calvo, E., Acin-Perez, R., Loureiro-Lopez, M., Pujol, C., Martinez-Carrascoso, I., Nunez, E., Garcia-Marques, F., Rodriguez-Hernandez, M. A., Cortes, A., Diaz, F., Perez-Martos, A., Moraes, C. T., Fernandez-Silva, P., Trifunovic, A., Navas, P., Vazquez, J. & Enriquez, J. A. (2016). The CoQH2/CoQ Ratio Serves as a Sensor of Respiratory Chain Efficiency. *Cell Rep,* 15**,** 197-209.
Hernández-Alvarez, M., Thabit, H., Burns, N., Shah, S., Brema, I., Hatunic, M., Finucane, F., Liesa, M., Chiellini, C. & Naon, D. (2010). Subjects with early-onset type 2 diabetes show defective activation of the skeletal muscle PGC-1α/mitofusin-2 regulatory pathway in response to physical activity. *Diabetes Care,* 33**,** 645-651.
Holloszy, J. O. (1967). Biochemical adaptations in muscle. Effects of exercise on mitochondrial oxygen uptake and respiratory enzyme activity in skeletal muscle. *J Biol Chem,* 242**,** 2278-82.
Jha, P., Wang, X. & Auwerx, J. (2016a). Analysis of Mitochondrial Respiratory Chain Supercomplexes Using Blue Native Polyacrylamide Gel Electrophoresis (BN-PAGE). *Curr Protoc Mouse Biol,* 6**,** 1-14.
Jha, P., Wang, X. & Auwerx, J. (2016b). Analysis of mitochondrial respiratory chain supercomplexes using blue native polyacrylamide gel electrophoresis (BN--PAGE). *Curr. Protoc. Mouse Biol,* 6**,** 1-14.
Kim, J. A., Wei, Y. & Sowers, J. R. (2008). Role of mitochondrial dysfunction in insulin resistance. *Circ Res,* 102**,** 401-14.
Konopka, A. R., Suer, M. K., Wolff, C. A. & Harber, M. P. (2014). Markers of human skeletal muscle mitochondrial biogenesis and quality control: effects of age and aerobic exercise training. *J Gerontol A Biol Sci Med Sci,* 69**,** 371-8.
Lanza, I. R., Short, D. K., Short, K. R., Raghavakaimal, S., Basu, R., Joyner, M. J., Mcconnell, J. P. & Nair, K. S. (2008). Endurance exercise as a countermeasure for aging. *Diabetes,* 57**,** 2933-42.
Lapuente-Brun, E., Moreno-Loshuertos, R., Acin-Perez, R., Latorre-Pellicer, A., Colas, C., Balsa, E., Perales-Clemente, E., Quiros, P. M., Calvo, E., Rodriguez-Hernandez, M. A., Navas, P., Cruz, R., Carracedo, A., Lopez-Otin,

C., Perez-Martos, A., Fernandez-Silva, P., Fernandez-Vizarra, E. & Enriquez, J. A. (2013). Supercomplex assembly determines electron flux in the mitochondrial electron transport chain. *Science,* 340**,** 1567-70.

Lombardi, A., Silvestri, E., Cioffi, F., Senese, R., Lanni, A., Goglia, F., De Lange, P. & Moreno, M. (2009). Defining the transcriptomic and proteomic profiles of rat ageing skeletal muscle by the use of a cDNA array, 2D- and Blue native-PAGE approach. *J Proteomics,* 72**,** 708-21.

Lopez-Lluch, G., Santos-Ocana, C., Sanchez-Alcazar, J. A., Fernandez-Ayala, D. J., Asencio-Salcedo, C., Rodriguez-Aguilera, J. C. & Navas, P. (2015). Mitochondrial responsibility in ageing process: innocent, suspect or guilty. *Biogerontology,* 16**,** 599-620.

Makrecka-Kuka, M., Krumschnabel, G. & Gnaiger, E. (2015). High-Resolution Respirometry for Simultaneous Measurement of Oxygen and Hydrogen Peroxide Fluxes in Permeabilized Cells, Tissue Homogenate and Isolated Mitochondria. *Biomolecules,* 5**,** 1319-38.

Maranzana, E., Barbero, G., Falasca, A. I., Lenaz, G. & Genova, M. L. (2013). Mitochondrial respiratory supercomplex association limits production of reactive oxygen species from complex I. *Antioxid Redox Signal,* 19**,** 1469-80.

Mckenzie, M., Lazarou, M., Thorburn, D. R. & Ryan, M. T. (2006). Mitochondrial respiratory chain supercomplexes are destabilized in Barth Syndrome patients. *J Mol Biol,* 361**,** 462-9.

Moreno-Lastres, D., Fontanesi, F., Garcia-Consuegra, I., Martin, M. A., Arenas, J., Barrientos, A. & Ugalde, C. (2012). Mitochondrial complex I plays an essential role in human respirasome assembly. *Cell Metab,* 15**,** 324-35.

Moreno-Loshuertos, R. & Enriquez, J. A. (2016). Respiratory supercomplexes and the functional segmentation of the CoQ pool. *Free Radic Biol Med*.

Mourier, A., Matic, S., Ruzzenente, B., Larsson, N. G. & Milenkovic, D. (2014). The respiratory chain supercomplex organization is independent of COX7a2l isoforms. *Cell Metab,* 20**,** 1069-75.

Muller, C. S., Bildl, W., Haupt, A., Ellenrieder, L., Becker, T., Hunte, C., Fakler, B. & Schulte, U. (2016). Cryo-slicing Blue Native-Mass Spectrometry (csBN-MS), a Novel Technology for High Resolution Complexome Profiling. *Mol Cell Proteomics,* 15**,** 669-81.

Perez-Perez, R., Lobo-Jarne, T., Milenkovic, D., Mourier, A., Bratic, A., Garcia-Bartolome, A., Fernandez-Vizarra, E., Cadenas, S., Delmiro, A., Garcia-Consuegra, I., Arenas, J., Martin, M. A., Larsson, N. G. & Ugalde, C. (2016). COX7A2L Is a Mitochondrial Complex III Binding Protein that Stabilizes the III2+IV Supercomplex without Affecting Respirasome Formation. *Cell Rep*.

Pesta, D. & Gnaiger, E. (2012). High-resolution respirometry: OXPHOS protocols for human cells and permeabilized fibers from small biopsies of human muscle. *Methods Mol Biol,* 810**,** 25-58.

Phielix, E., Meex, R., Moonen-Kornips, E., Hesselink, M. K. & Schrauwen, P. (2010). Exercise training increases mitochondrial content and ex vivo mitochondrial function similarly in patients with type 2 diabetes and in control individuals. *Diabetologia,* 53**,** 1714-21.

Safdar, A., Hamadeh, M., Kaczor, J., Raha, S. & Tarnopolsky, M. (2010). Aberrant mitochondrial homeostasis in the skeletal muscle of sedentary older adults. *PLoS One,* 5**,** e10778.

Schagger, H. (2002). Respiratory chain supercomplexes of mitochondria and bacteria. *Biochim Biophys Acta,* 1555**,** 154-9.

Schagger, H., De Coo, R., Bauer, M. F., Hofmann, S., Godinot, C. & Brandt, U. (2004). Significance of respirasomes for the assembly/stability of human respiratory chain complex I. *J Biol Chem,* 279**,** 36349-53.

Schagger, H. & Pfeiffer, K. (2000). Supercomplexes in the respiratory chains of yeast and mammalian mitochondria. *EMBO J,* 19**,** 1777-83.

Short, K. R., Bigelow, M. L., Kahl, J., Singh, R., Coenen-Schimke, J., Raghavakaimal, S. & Nair, K. S. (2005). Decline in skeletal muscle mitochondrial function with aging in humans. *Proc Natl Acad Sci USA,* 102**,** 5618-23.

Sun, D., Li, B., Qiu, R., Fang, H. & Lyu, J. (2016). Cell Type-Specific Modulation of Respiratory Chain Supercomplex Organization. *Int J Mol Sci,* 17.

Ugalde, C., Janssen, R. J., Van Den Heuvel, L. P., Smeitink, J. A. & Nijtmans, L. G. (2004). Differences in assembly or stability of complex I and other mitochondrial OXPHOS complexes in inherited complex I deficiency. *Hum Mol Genet,* 13**,** 659-67.

Vempati, U. D., Han, X. & Moraes, C. T. (2009). Lack of cytochrome c in mouse fibroblasts disrupts assembly/stability of respiratory complexes I and IV. *J Biol Chem,* 284**,** 4383-91.

Williams, E. G., Wu, Y., Jha, P., Dubuis, S., Blattmann, P., Argmann, C. A., Houten, S. M., Amariuta, T., Wolski, W., Zamboni, N., Aebersold, R. & Auwerx, J. (2016). Systems proteomics of liver mitochondria function. *Science,* 352**,** aad0189.

TABLES

Table 1. Subject's characteristics

Subjects N=26 15 females/11 males	Pre-intervention	Post-intervention	P-Value
Age (years)	65.86 ± 0.68 [60-72]		
BMI (kg/m^2)	26.84 ± 0.94 [17.75-37.02]	26.48 ± 0.88 [17.75-35.77]	**0.01**
$\dot{V}O_2$ peak (l/min)	1.91 ± 0.09 [1.26-2.59]	2.15 ± 0.10 [1.32-3.32]	**<.0001**
Mitochondria volume density (%)	5.06 ± 0.27 [2.85-8.69]	6.92 ± 0.34 [3.46-9.48]	**<.0001**

Values are Mean ± SEM [min-max]. $\dot{V}O_2$ peak is peak oxygen consumption. P-value from Paired T test (2 tails).

Table 2. Relationship between post-intervention changes in electron transport chain complexes (free or SC $I+III_2+IV_n$ superassembled pools) and changes in exercise capacity, efficiency and reliance on fat during an acute bout of exercise

Change in (%)	**Peak oxygen uptake**	**Exercise efficiency**	**Exercise fat oxidation**
CI in SC $I+III_2+IV_n$	0.10	-0.5	0.25
CIII in SC $I+III_2+IV_n$	0.67*	0.29	0.5
Free CIII	-0.71*	-0.15	-0.75*
CIV in SC $I+III_2+IV_n$	-0.03	0.76*	0.03
Free CIV	0.35	-0.71*	0.30

N=9, Values are Spearman's Rank-Order correlation coefficient rho. *p-value<0.05.

Table 3. Relationship between oxygen fluxes measured by high resolution respirometry and supercomplexes content, including relative proportions of free or superassembled complexes

	O_2 flux (pmol/s/mg tissue)			
	CI linked	**CII linked**	**CI&II linked**	**Leak**
SC I+III$_2$+IV$_n$ (A.U.)	0.68	0.49	0.76*	-0.74¶
CI in SCs (A.U.)	0.68	0.50	0.76*	-0.74¶
CIII in SCs (A.U.)	0.64	0.45	0.71	-0.74¶
Proportion of CIII in SCs (%)	*0.48*	*0.27*	*0.53*	*-0.83**
Proportion of free CIII (%)	*-0.48*	*-0.27*	*-0.53*	*0.83**
CIV in SCs (A.U.)	0.85*	0.38	0.90**	-0.66
CIV in SC I+III$_2$+IV$_n$ (A.U.)	0.78*	0.42	0.84*	-0.73¶
CIV in SC III$_2$+IV (A.U.)	0.87*	0.16	0.91*	-0.03
Proportion of CIV in SCs (%)	*0.80**	*0.45*	*0.87**	*-0.71#*
Proportion of CIV in SC I+III$_2$+IV$_n$ (%)	*0.68#*	*0.50*	*0.76**	*-0.75**
Proportion of CIV in SC III$_2$+IV (%)	*0.91***	*0.25*	*0.93***	*-0.47*
Proportion of free CIV (%)	*-0.86**	*-0.51*	*-0.94***	*0.71#*

Pearson correlation coefficients, *P<0.05, ** P<0.005, ¶P=0.06, #P<0.1. In *italics*, proportion of relative content of the different complexes that are either in free form or superassembled. SCs is the sum of all supercomplexes containing that particular complex. Respirometry nomenclature was defined based on the blue book from Gnaiger (Gnaiger, 2014a) and the MitoPedia network (Gnaiger, 2014b).

FIGURES LEGENDS

Fig 1. **Exercise increases individual ETC complexes in older skeletal muscle.** (A) Protein content of each individual complex was quantified by western blotting from whole muscle lysate from *vastus lateralis* biopsies. A representative western blot is included with pre- and post- intervention bands for the five complexes and loading control. (B) Changes in individual complexes with 16-wk of exercise. Post-intervention content was normalized over its respective baseline content (dashed red line). For CI, n=23; for CII, CIII, and CV, n= 24; for CIV, n= 19. Black lines are mean and SD. *p<0.05. (C) Percent change of CI with intervention was not correlated with percent change of CII, CIII and CIV. (D) Percent change in CII was related to changes in CIII and CIV. Percent change in CIII was related with changes in CIV. (E) Relative mRNA abundance for CI (*NDUFA2*) and CV (*ATP5G1*) pre and post-intervention. Black lines are mean and SD. *p<0.05.

Fig 2. **Exercise increases SCs abundance.** (A) Representative BN-PAGE experiment with mitochondrial extracts from one human skeletal muscle. Specific antibodies against individual ETC complexes were used separately. The high molecular weight bands (10), labeled high molecular weight SCs (HMW SCs), were mainly composed of SC I_n+III_n and V_n. Also included in HMW SCs is a light smear on CIV corresponding to bands in CI and CIII identified as SC I+III_2+IV_n. The strong bands composed of I, III and IV were defined as SC I+III_2+IV (9). Band 8 was identified as SC I+III_2. Four intense bands (7, 6, 5 and 3) were composed of oligomeric chains of CV, labeled V_n. (Specific species interpretations may include F1V_2 for band 6, the monomer V_1 for band 5 and F1 for band 3). Band 5 was identified as SC III_2+IV co-migrated with V_n. Band 4 was identified as III_2 and co-migrated with a weak CIV dimer IV_2. CIV was identified in band 2, while band 1

consisted of CII. (B) BN-PAGE before and after the 16-week exercise training (n=17). For quantification of the total amount of “SCs”, the signals corresponding to bands > ≈1,000 kDa were used. SC III_2+IV was not included due to our incapacity to disentangle this particular SC from the co-migrated complex V. (C) Quantification of SCs changes with intervention. Post-intervention SCs content for each subject (N=17) was normalized over its own pre-intervention content (red dashed line). Black lines are mean and SD. *p<0.05.

Fig 3. **Exercise promotes ETC complexes redistribution** (N=9). (A) Exercise significantly increased CI, CIII, CIV positive SCs. Post-intervention content was normalized over its respective baseline content (dashed red line). Black lines are mean and SD. *p<0.05. (B) Effect of intervention on superassembled fractions of ETC complexes. At baseline, >95% of CI was in SCs, suggesting that only traces of CI were in the free form in sedentary human muscle. This distribution did not change with exercise. At baseline >40% of CIII was in the free pool. The % of superassembled CIII increased after intervention. At baseline >80% of CIV was in the free form. The superassembled fraction of CIV increased after intervention. Black lines are mean and SD. *p<0.05. (C) Exercise significantly affected the distribution of ETC complexes into SCs (“<” pre<post; “>” pre>post, p<0.05, ϕ p=0.06). Representative BN-PAGE experiments on mitochondrial extracts from human skeletal muscle biopsies before and after intervention show annotations of the different quantified species. Bars are mean, error bars are SD. (D) Correlations between free and superassembled fractions. The inverse correlation between changes in free and superassembled fractions for CIII and CIV are suggestive of an incorporation of the free complexes in SCs. The decreased incorporations of CI and CIII in SC I+III_2 fraction are positively associated. (E) Relationships between exercise

outcomes and SCs. Overall content of CIII in SCs was positively correlated to peak oxygen uptake (VO_2peak). Overall content of CIV in SCs and CIV in SC I+III_2+IV_n followed a similar relationship. Free CIV was inversely correlated with VO_2peak**.** CIV in SCs was positively correlated to exercise efficiency adjusted to leg mass (adjusted GE). Free CIV was inversely correlated with adjusted GE. CIII superassembled in SC I+III_2+IV_n was positively related to the amount of fat oxidized during one bout of steady state exercise, and thus to reliance on energy coming from fat during exercise.

Fig 4. **Mitochondrial respiration is related to SCs abundance in human skeletal muscle.** (A) High resolution respirometry in permeabilized fibers from muscle biopsies (N=7). Leak, also known as state 2 - CI respiration, corresponds to the dissipative component of respiration. CI linked is complex I linked O_2 flux (State 3 - CI). CI&II linked is complex I and II linked O_2 flux (state 3 – CI+CII). Electron transfer system capacity (ETS) is for maximal respiration, which represents maximal O_2 flux. ROX is the residual O_2 consumption. (B) Flux control ratios (FCR) normalized to ETS from Leak, CI and CII linked O_2 fluxes corrected for ROX. (C) BN-PAGE of mitochondrial extracts from the same muscle biopsies. L is mice liver for labeling and comparison. (D) ECL detection of relative distribution of CI, CIII and CIV in free or superassembled complexes (SCs). CI and CIII in SCs correspond to the overlap of SC I+III_2+IV_n and SC I+III_2. E) Maximal O_2 flux (ETS) as a function of the overall content of SC I+III_2+IV_n and of the amount of CI, CIII and CIV in overall or specific SCs. CIV in SCs represents the sum of CIV in SC I+III_2+IV_n and SC III_2+IV. For all panels, bars are mean, error bars are SEM. *P<0.05, **P<0.005, ¶=0.06.

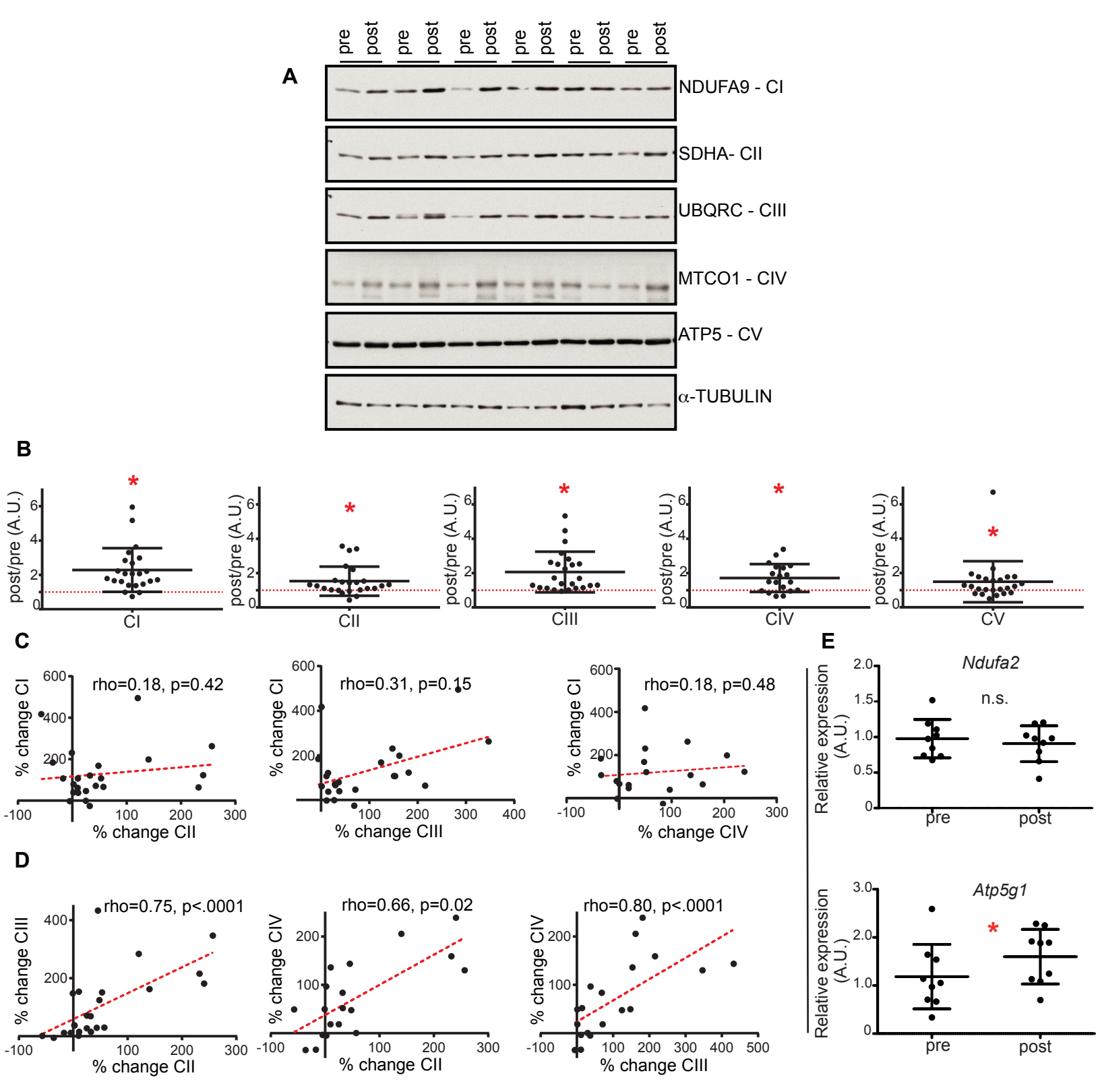
A
pre
post
NDUFA9 - CI
SDHA- CII
UBQRC - CIII
MTCO1 - CIV
ATP5 - CV
α-TUBULIN
B
post/pre (A.U.)
CI
CII
CIII
CIV
CV
C
rho=0.18, p=0.42
% change CI
% change CII
rho=0.31, p=0.15
% change CIII
rho=0.18, p=0.48
% change CIV
D
rho=0.75, p<.0001
% change CIII
% change CII
rho=0.66, p=0.02
% change CIV
% change CII
rho=0.80, p<.0001
% change CIV
% change CIII
E
Ndufa2
n.s.
Relative expression (A.U.)
pre
post
Atp5g1
Relative expression (A.U.)
pre
post

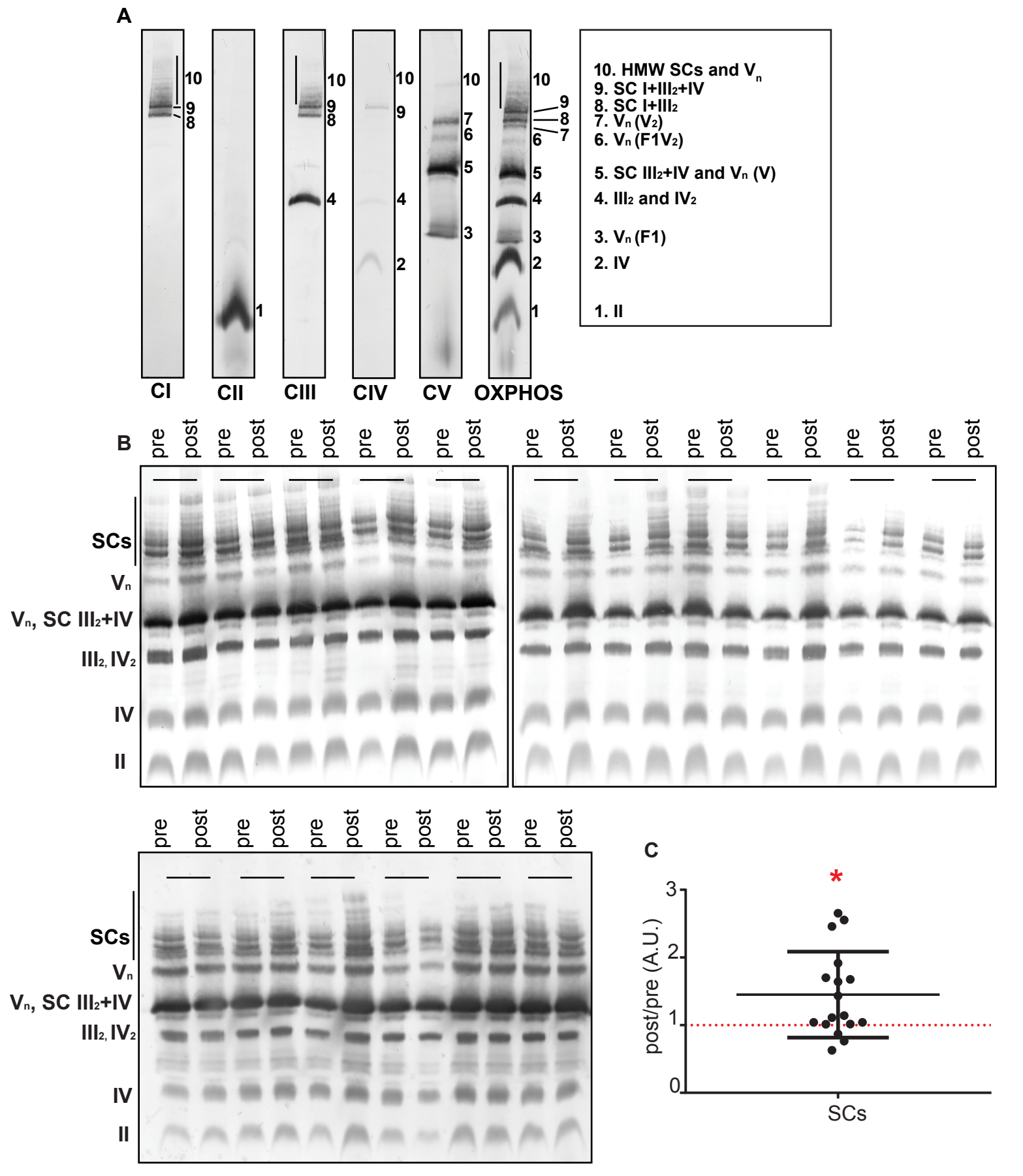
A
10
9
8
1
CI
10
9
8
CII
10
9
4
CIII
10
9
2
CIV
10
7
6
5
3
CV
10
9
8
7
6
5
4
3
2
1
OXPHOS
10. HMW SCs and Vn
9. SC I+III2+IV
8. SC I+III2
7. Vn (V2)
6. Vn (F1V2)
5. SC III2+IV and Vn (V)
4. III2 and IV2
3. Vn (F1)
2. IV
1. II
B
pre
post
SCs
Vn
Vn, SC III2+IV
III2, IV2
IV
II
C
post/pre (A.U.)
3
2
1
0
*
SCs

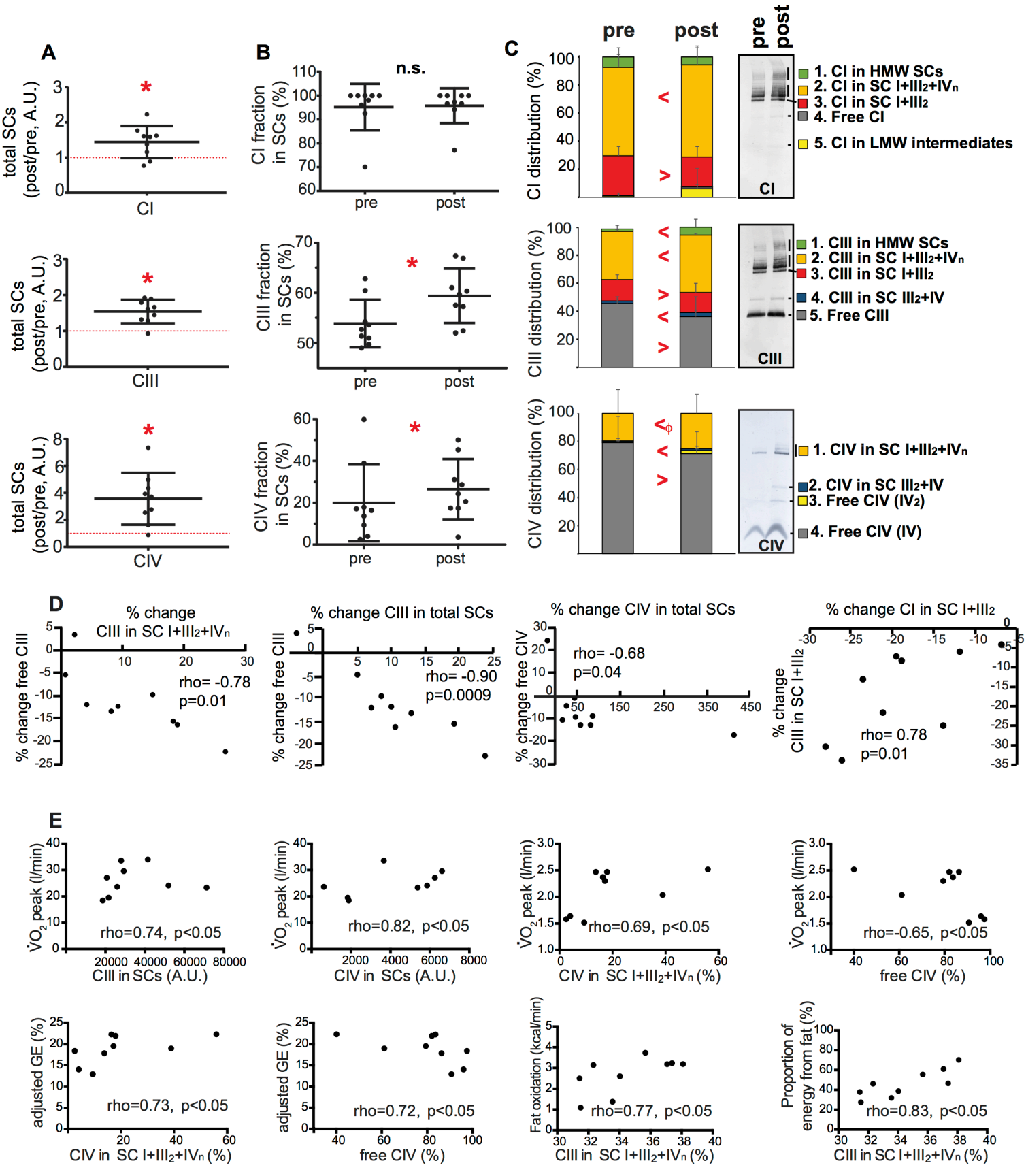
A
total SCs (post/pre, A.U.)
CI
CIII
CIV
B
n.s.
CI fraction in SCs (%)
CIII fraction in SCs (%)
CIV fraction in SCs (%)
pre
post
C
pre
post
CI distribution (%)
CIII distribution (%)
CIV distribution (%)
1. CI in HMW SCs
2. CI in SC I+III2+IVn
3. CI in SC I+III2
4. Free CI
5. CI in LMW intermediates
1. CIII in HMW SCs
2. CIII in SC I+III2+IVn
3. CIII in SC I+III2
4. CIII in SC III2+IV
5. Free CIII
1. CIV in SC I+III2+IVn
2. CIV in SC III2+IV
3. Free CIV (IV2)
4. Free CIV (IV)
D
% change CIII in SC I+III2+IVn
% change CIII in total SCs
% change CIV in total SCs
% change CI in SC I+III2
% change free CIII
% change free CIV
% change CIII in SC I+III2
rho= -0.78
p=0.01
rho= -0.90
p=0.0009
rho= -0.68
p=0.04
rho= 0.78
p=0.01
E
VO2 peak (l/min)
rho=0.74, p<0.05
CIII in SCs (A.U.)
rho=0.82, p<0.05
CIV in SCs (A.U.)
rho=0.69, p<0.05
CIV in SC I+III2+IVn (%)
rho=-0.65, p<0.05
free CIV (%)
adjusted GE (%)
rho=0.73, p<0.05
CIV in SC I+III2+IVn (%)
rho=0.72, p<0.05
free CIV (%)
Fat oxidation (kcal/min)
rho=0.77, p<0.05
CIII in SC I+III2+IVn (%)
Proportion of energy from fat (%)
rho=0.83, p<0.05
CIII in SC I+III2+IVn (%)

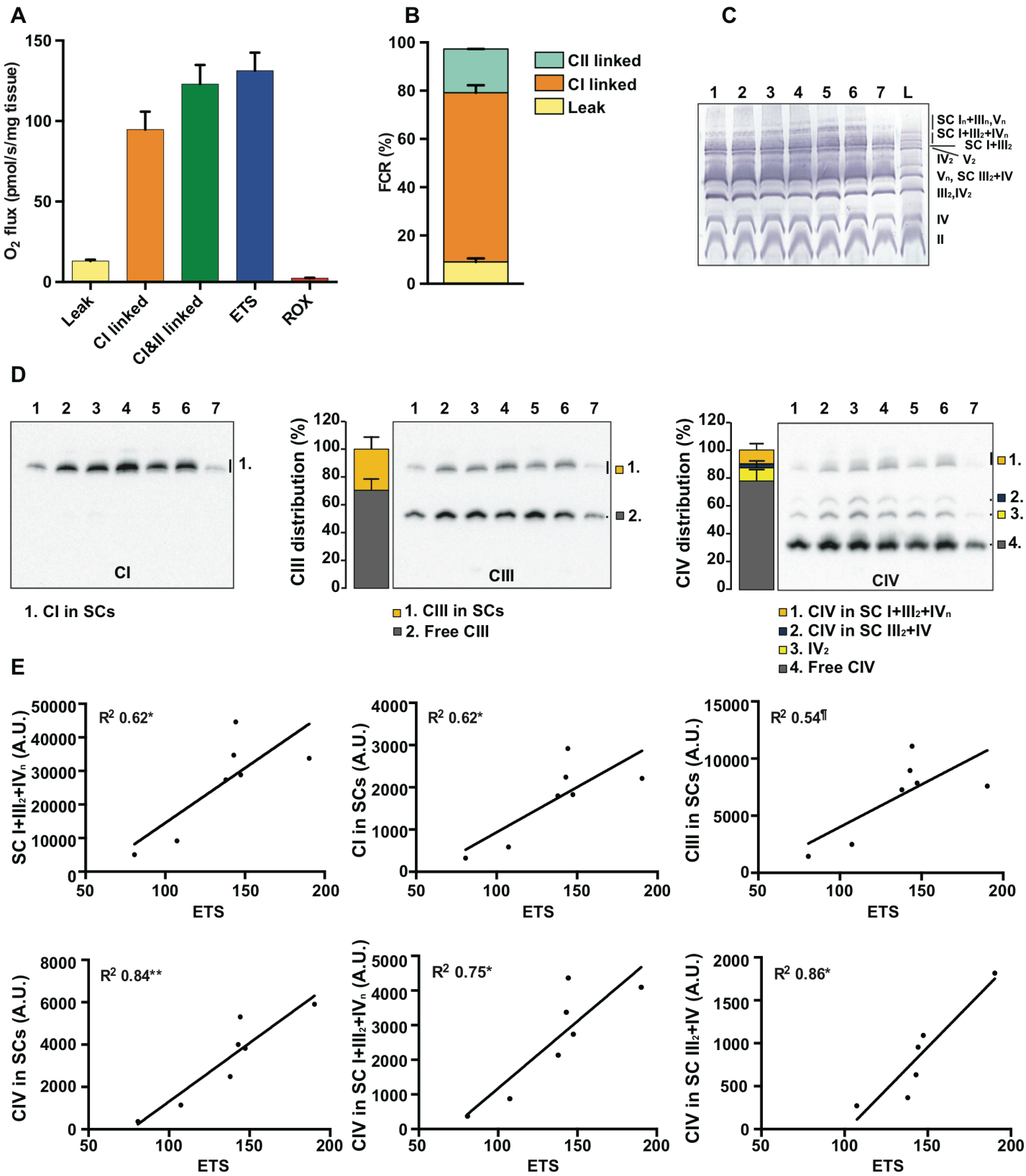
A
O2 flux (pmol/s/mg tissue)
150
100
50
0
Leak
CI linked
CI&II linked
ETS
ROX
B
FCR (%)
100
80
60
40
20
0
CII linked
CI linked
Leak
C
1 2 3 4 5 6 7 L
SC In+IIIn,Vn
SC I+III2+IVn
SC I+III2
IV2 V2
Vn, SC III2+IV
III2,IV2
IV
II
D
1 2 3 4 5 6 7
1.
CI
1. CI in SCs
CIII distribution (%)
120
100
80
60
40
20
0
CIII
1. CIII in SCs
2. Free CIII
CIV distribution (%)
CIV
1. CIV in SC I+III2+IVn
2. CIV in SC III2+IV
3. IV2
4. Free CIV
E
SC I+III2+IVn (A.U.)
R2 0.62*
CI in SCs (A.U.)
R2 0.62*
CIII in SCs (A.U.)
R2 0.54¶
CIV in SCs (A.U.)
R2 0.84**
CIV in SC I+III2+IVn (A.U.)
R2 0.75*
CIV in SC III2+IV (A.U.)
R2 0.86*
ETS

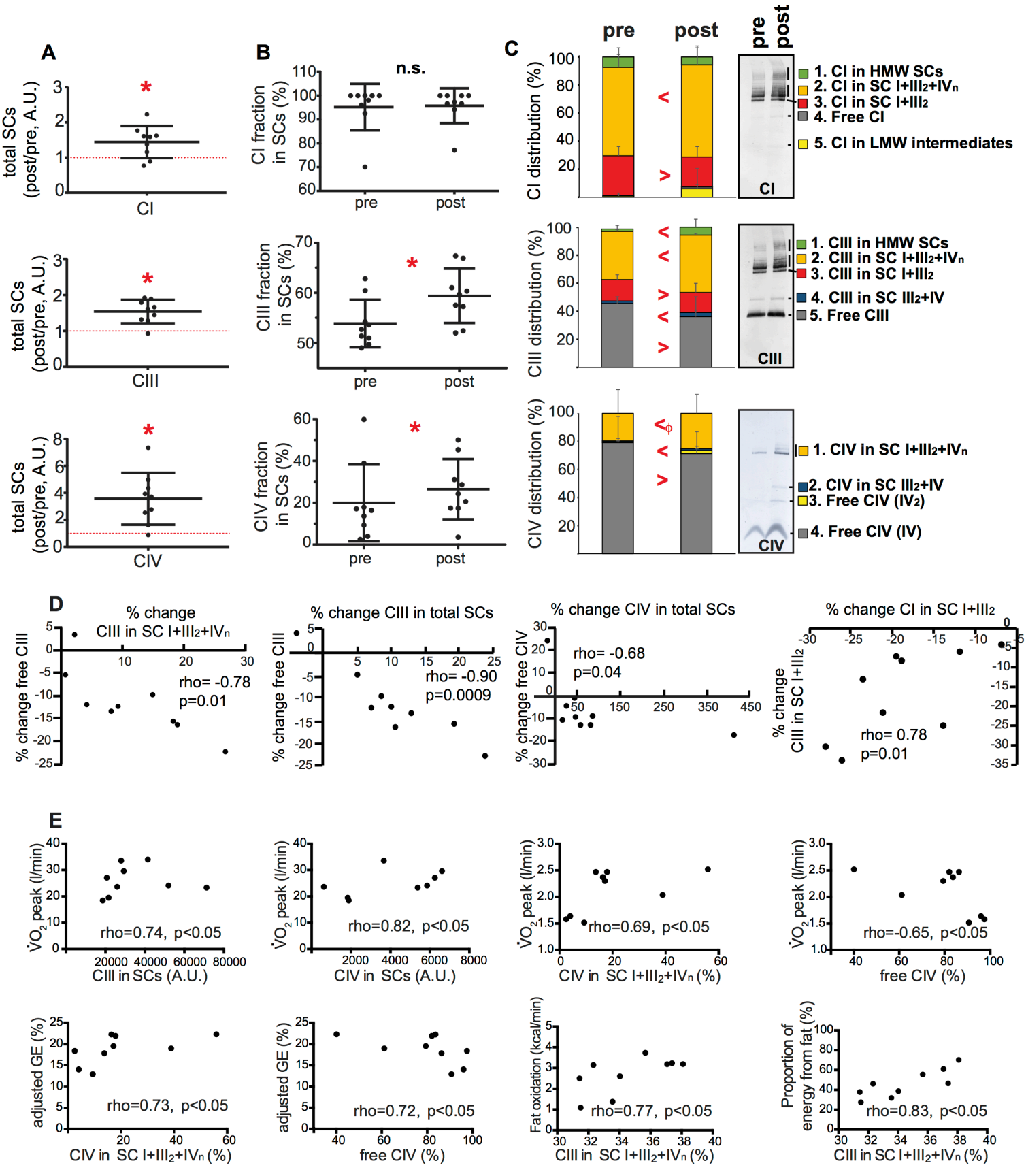
A
total SCs (post/pre, A.U.)
CI
CIII
CIV
B
n.s.
CI fraction in SCs (%)
CIII fraction in SCs (%)
CIV fraction in SCs (%)
pre
post
C
pre
post
CI distribution (%)
CIII distribution (%)
CIV distribution (%)
1. CI in HMW SCs
2. CI in SC I+III2+IVn
3. CI in SC I+III2
4. Free CI
5. CI in LMW intermediates
1. CIII in HMW SCs
2. CIII in SC I+III2+IVn
3. CIII in SC I+III2
4. CIII in SC III2+IV
5. Free CIII
1. CIV in SC I+III2+IVn
2. CIV in SC III2+IV
3. Free CIV (IV2)
4. Free CIV (IV)
D
% change CIII in SC I+III2+IVn
% change CIII in total SCs
% change CIV in total SCs
% change CI in SC I+III2
% change free CIII
% change free CIV
% change CIII in SC I+III2
rho= -0.78
p=0.01
rho= -0.90
p=0.0009
rho= -0.68
p=0.04
rho= 0.78
p=0.01
E
VO2 peak (l/min)
rho=0.74, p<0.05
CIII in SCs (A.U.)
rho=0.82, p<0.05
CIV in SCs (A.U.)
rho=0.69, p<0.05
CIV in SC I+III2+IVn (%)
rho=-0.65, p<0.05
free CIV (%)
adjusted GE (%)
rho=0.73, p<0.05
CIV in SC I+III2+IVn (%)
rho=0.72, p<0.05
free CIV (%)
Fat oxidation (kcal/min)
rho=0.77, p<0.05
CIII in SC I+III2+IVn (%)
Proportion of energy from fat (%)
rho=0.83, p<0.05
CIII in SC I+III2+IVn (%)

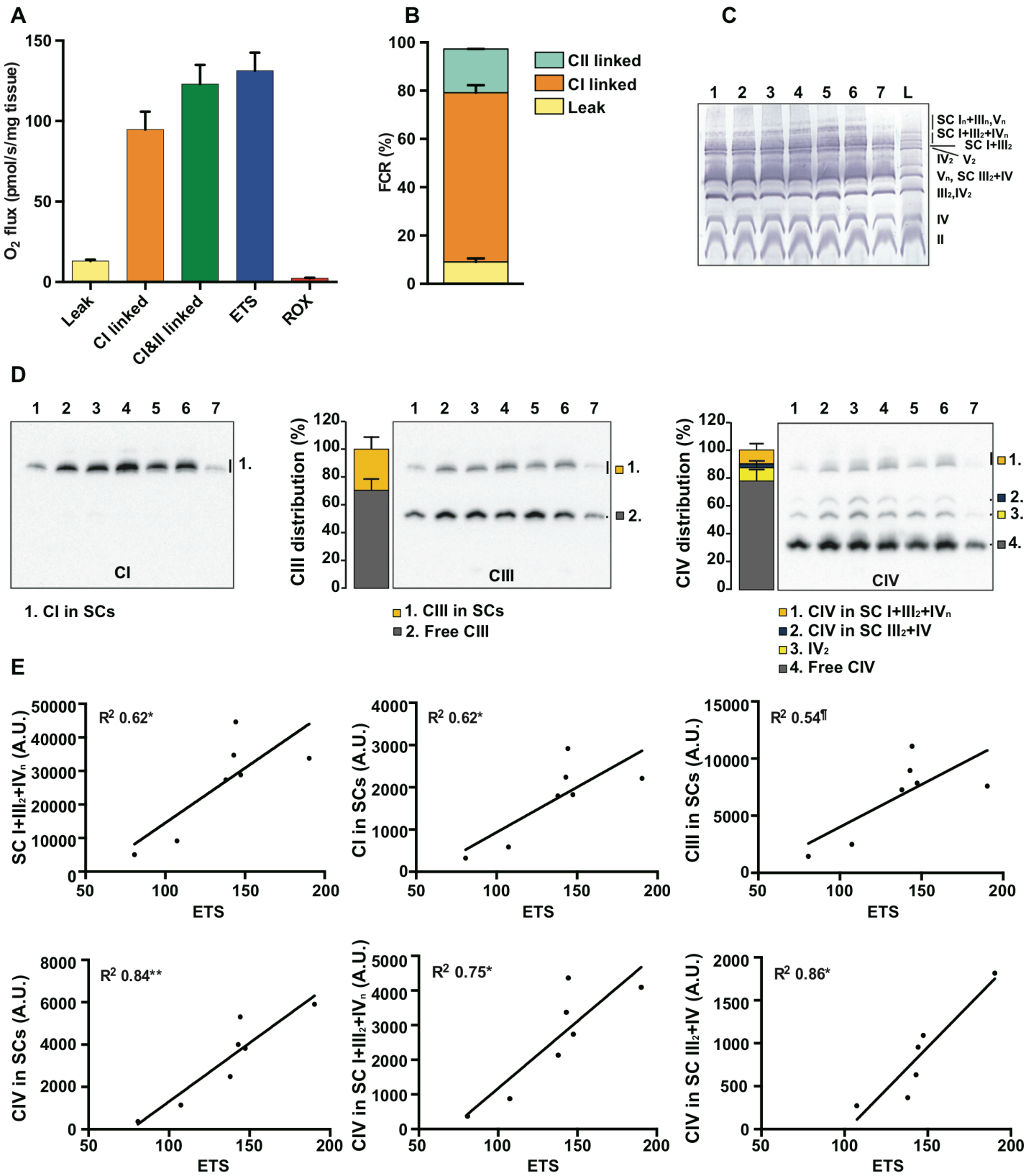
A
O2 flux (pmol/s/mg tissue)
150
100
50
0
Leak
CI linked
CI&II linked
ETS
ROX
B
FCR (%)
100
80
60
40
20
0
CII linked
CI linked
Leak
C
1 2 3 4 5 6 7 L
SC In+IIIn,Vn
SC I+III2+IVn
SC I+III2
IV2 V2
Vn, SC III2+IV
III2,IV2
IV
II
D
1 2 3 4 5 6 7
1.
CI
1. CI in SCs
CIII distribution (%)
120
100
80
60
40
20
0
CIII
1. CIII in SCs
2. Free CIII
CIV distribution (%)
CIV
1. CIV in SC I+III2+IVn
2. CIV in SC III2+IV
3. IV2
4. Free CIV
E
SC I+III2+IVn (A.U.)
R2 0.62*
CI in SCs (A.U.)
R2 0.62*
CIII in SCs (A.U.)
R2 0.54¶
CIV in SCs (A.U.)
R2 0.84**
CIV in SC I+III2+IVn (A.U.)
R2 0.75*
CIV in SC III2+IV (A.U.)
R2 0.86*
ETS

Supplemental material

CONTENT

SUPPLEMENTAL FIGURES

Figure S1

A

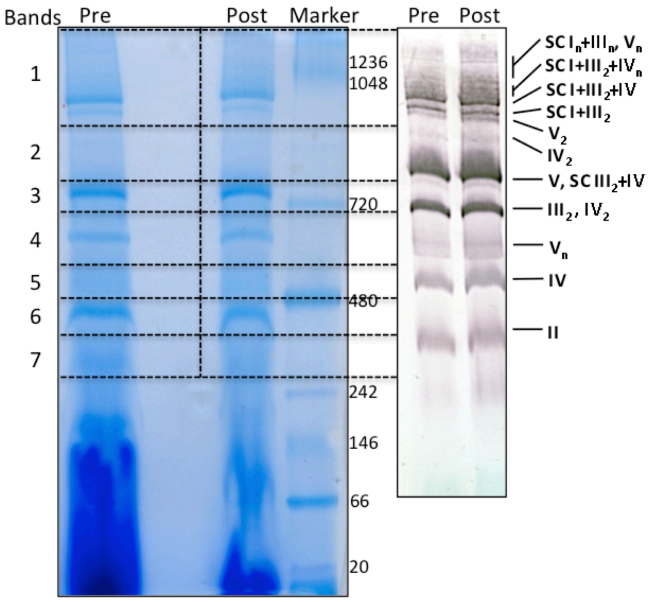

B

Bands	Sample	CI	CII	CIII	CIV	CV
1: All SCs, IV2, V2	Pre	36	–	8	12	13
	Post	36	–	8	12	13
2: I; V; III2+IV	Pre	6	-	6	10	17
	Post	6	-	6	10	17
3: III2; IV2	Pre	–	-	7	12	17
	Post	–	-	7	12	17
4: Vn	Pre	-	-	8	11	15
	Post	-	-	8	11	15
5: IV	Pre	-	-	-	11	12
	Post	-	-	-	11	12
6: II; IV	Pre	-	1	-	17	1
	Post	-	1	-	16	1
7: II	Pre	1	3	-	-	1
	Post	1	3	-	-	1

Expected position of the proteins corresponding to the band position
Unexpected position of the proteins due to cutting overlap
proteins for which peptide count is 50% of the max.
– =Protein undetected/ peptide count less than 50% of the max.

Figure S2

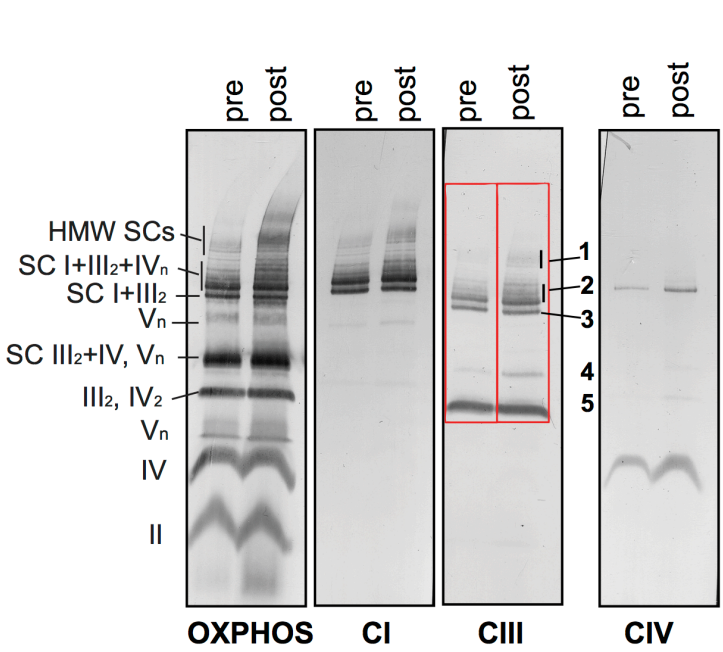

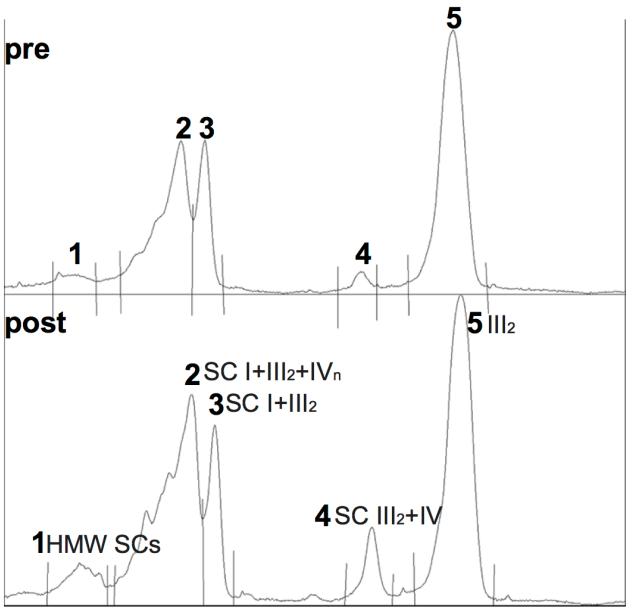

Figure S3

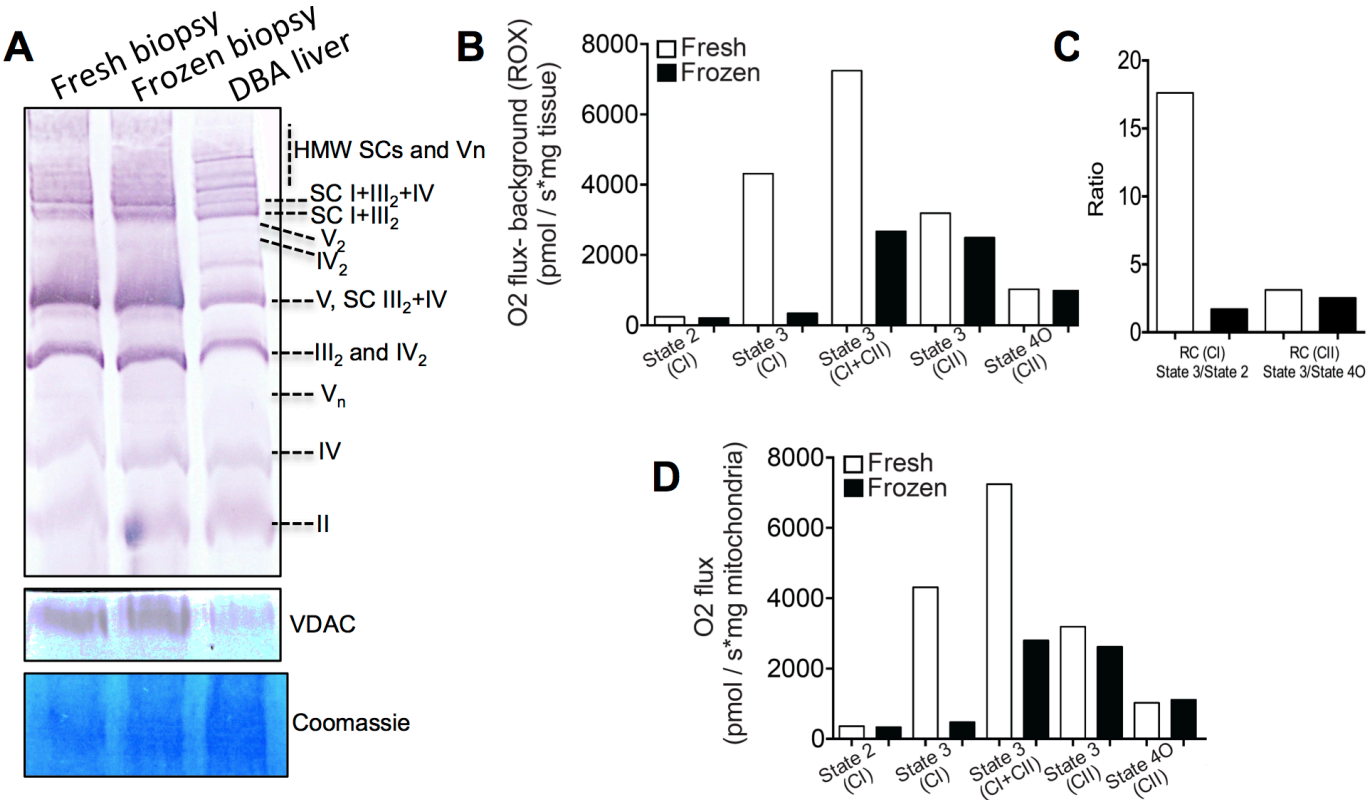

Figure S4

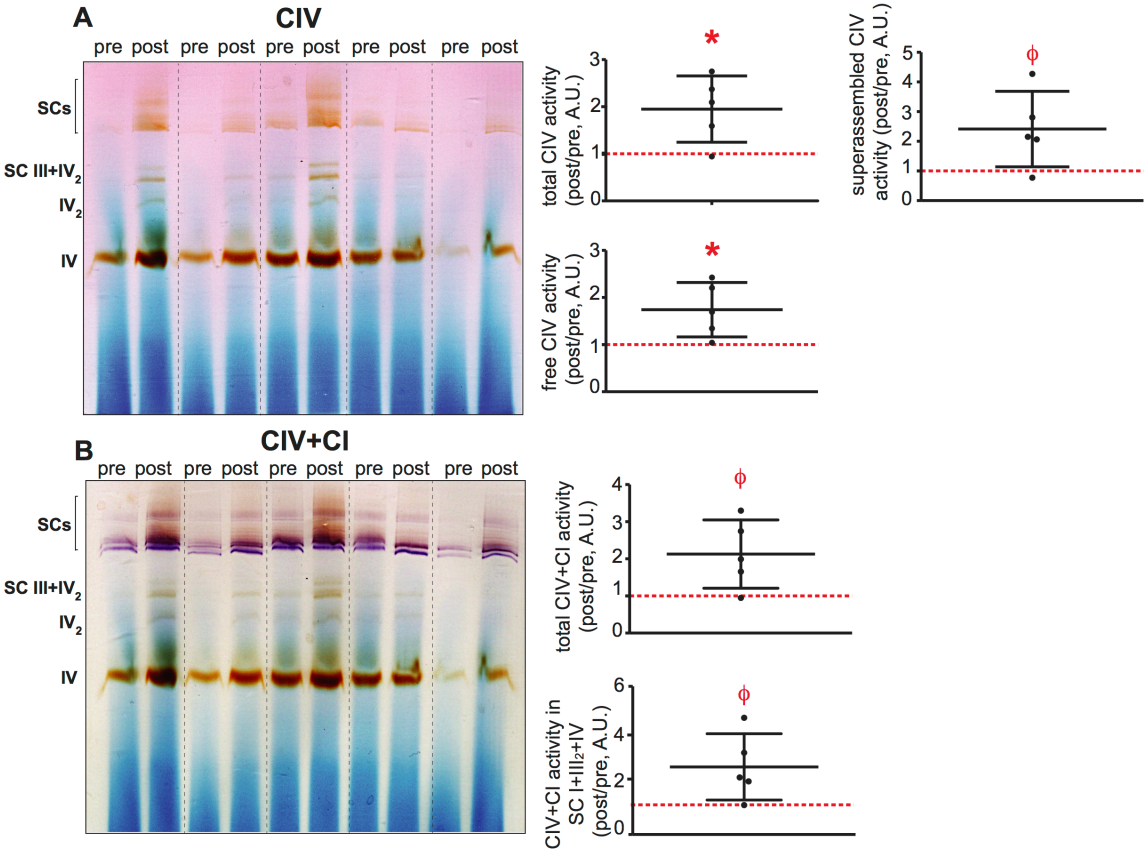

SUPPLEMENTAL FIGURES LEGENDS

Figure S1: Proteomics analysis of the BN-PAGE bands (related to Figure 2). (A) 100µg of protein at a concentration of 8g protein/g digitonin were run on BN-PAGE for 3h (30 min at 150V and 150 min at 250 V). 7 bands were cut, as indicated in the figure. The bands were then processed for LC-MS based proteomic profiling. (B) Number of proteins corresponding to each complex present in the respective band.

Figure S2: Quantification of CI, CIII, CIV SCs (related to figure 3). Example of quantification for one subject before and after intervention. Using ImageJ (Analyze-Gels-Plot lanes), individual peaks for each complex were quantified as singlets and, when applicable, also summed as "total SCs". In this specific case, for example, the CIII signal was distributed in 5 peaks, of which (1+2+3+4) were used as "CIII in total SCs". Due to the shape of peak 2, SC I+III_2+IV was included within SC I+III_2+IV_n.

Figure S3: Supercomplex stoichiometry is maintained in frozen samples, despite respiration being compromised (related to figure 4). (A) BN-PAGE profile comparison between mitochondria extracts from fresh and frozen muscle show the same stoichiometry. (B) Oxygen consumption from fresh and frozen muscle shows highly compromised complex I activity in frozen samples. (C) Respiratory coupling (RC) of fresh and frozen muscle shows a large loss of efficiency of CI. (D) Oxygen consumption of mitochondria extracts from fresh and frozen muscle shows the same pattern as whole muscle and confirms that the extraction protocol produces functional mitochondria.

Figure S4: In gel activity of specific ETC complexes in SCs (related to experimental procedure BN-PAGE in gel activity assays). (A) In-gel activity for CIV was measured in mitochondrial extracts from human skeletal muscle biopsies before and after intervention (n=5). Post-intervention activity for each subject was normalized over its own pre-intervention content (defined as 1, red dashed line). In response to exercise, significant increases in CIV activity were observed. (B) In-gel activity for CI was measured after CIV detection. The cumulative signals from CI and CIV activities tended to increase in response to exercise and the same was true for the activity detected in the CI positive SCs. Similar protein loadings in "pre-post" samples were confirmed by Coomassie Blue staining. Data are mean and SD. *$p<0.05$; ϕ $p= 0.05$-0.07.

SUPPLEMENTAL TABLE

Table S1. Baseline correlations between individual ETC complexes (related to figure 1). Expression of individual complexes in human skeletal muscle was measured by western blotting in sedentary conditions (i.e. before intervention). Relative amounts of CI and CII were not related to each other. CI and CII were positively associated with CIII and CIV, which in turn correlated to each other. CV was related only with CII at baseline.

	CI	**CII**	**CIII**	**CIV**	**CV**
CI	-	0.32 p=0.13	**0.65** **p=0.0006**	**0.50** **p=0.03**	0.30 p=0.16
CII		-	**0.65** **p=0.0006**	**0.66** **p=0.002**	**0.65** **p=0.0006**
CIII			-	**0.76** **p=0.0002**	0.31 p=0.14
CIV				-	0.24 p=0.32
CV					-

ETC complexes measured by WB normalized by α-tubulin. Values are Spearman's Rank-Order correlation coefficient rho and p-values.

SUPPLEMENTAL METHODS

Proteomic analysis

Sections of coomassie-stained gel lanes were excised and digested with trypsin (Promega) as described (Wilm et al., 1996, Shevchenko et al., 1996). Data-dependent LC-MS/MS analysis of extracted peptide mixtures after digestion with trypsin was carried out on a hybrid linear trap LTQ-Orbitrap Velos Pro mass spectrometer (Thermo Fisher Scientific) interfaced to a nanocapillary HPLC (Dionex RSLC 3000) equipped with a C18 reversed-phase column. Collections of peptide tandem mass spectra were searched using Mascot 2.5.1 (Matrix Science, London, UK) against the December 2015 release of the human proteome set of sequences from the UNIPROT database (SWISSPROT + TrEMBL, www.expasy.org). The software Scaffold (version 4.4.8, Proteome Software Inc.) was used to validate MS/MS based peptide (minimum 90% probability (Keller et al., 2002) and protein (min 95 % probability (Nesvizhskii et al., 2003)) identifications, perform dataset alignment as well as parsimony analysis to discriminate homologous hits.

REFERENCES

Keller, A., Nesvizhskii, A. I., Kolker, E. & Aebersold, R. (2002). Empirical statistical model to estimate the accuracy of peptide identifications made by MS/MS and database search. *Anal Chem,* 74**,** 5383-92.

Nesvizhskii, A. I., Keller, A., Kolker, E. & Aebersold, R. (2003). A statistical model for identifying proteins by tandem mass spectrometry. *Anal Chem,* 75**,** 4646-58.

Shevchenko, A., Wilm, M., Vorm, O. & Mann, M. (1996). Mass spectrometric sequencing of proteins silver-stained polyacrylamide gels. *Anal Chem,* 68**,** 850-8.

Wilm, M., Shevchenko, A., Houthaeve, T., Breit, S., Schweigerer, L., Fotsis, T. & Mann, M. (1996). Femtomole sequencing of proteins from polyacrylamide gels by nano-electrospray mass spectrometry. *Nature,* 379**,** 466-9.